

# Chapter 1

## Two Quark Potentials

G. Bali

*Department of Physics & Astronomy, University of Glasgow,  
Glasgow G12 8QQ, Scotland  
E-mail: g.bali@physics.gla.ac.uk*

In this Chapter QCD interactions between a quark and an anti-quark are discussed. In the heavy quark limit these potentials can be related to quarkonia and  $1/m$  corrections can be systematically determined. Excitations of the ground state potential provide an entry point into the phenomenology of quark-gluon hybrids. The short-distance behaviour of non-perturbative potentials can serve as a test of resummation and convergence of perturbative expansions. Torelons and potentials between non-fundamental colour charges offer a window into the origin of the confinement mechanism and relate to effective string descriptions of low energy aspects of QCD.

### 1.1 Motivation

In order to avoid excessive overlap with the many introductions that already exist in different places of this Volume, we shall elaborate on a very subjective motivation of studying interquark potentials in QCD, centred around the general theme of *building bridges* between models and QCD.

QCD contains two related, non-perturbative features: the breaking of (approximate) chiral symmetry and the (effective) confinement of coloured objects such as quarks and gluons. Similarly, models of the QCD vacuum can roughly be divided into two classes: those that are primarily based on chiral symmetry and those that have confinement, for instance in the form of a confining potential, as their starting point. Often it is difficult to *microscopically* relate a particular model to QCD. For example, should the instantons that are evidenced in lattice simulations within a given pre-

scription at a finite cut-off, be the same that are supposed to appear within instanton liquid models? The answer to this question is not known.

There exist, however, two ways of systematically *building bridges*. Perhaps the most obvious one is the comparison of *global* properties like form factors, charge distributions in position space, potential energies or particle masses. Such a comparison circumvents the problem of identifying a one-to-one mapping of the degrees of freedom within a given model, which often might not qualify as a quantum field theory, onto objects that appear in the QCD vacuum. The model would then very much resemble the pragmatic use of analogies in the popular science literature: it is not that important to get things 100 % right if we cannot understand them 100 % anyway.

A lot of purpose-engineered QCD information that is not directly accessible to experiment can be *manufactured* in lattice simulations. Moreover, in experiment there is only one world. On the lattice one has the freedom to vary the number of sea quark flavours  $n_f$ , the quark masses, the number of gauge group colours,  $N_C$ , the volume *etc. etc.*, away from the values that happen to be realized in nature for one reason or another. Sometimes (like in the case of quark masses) this is at present a necessity, in other cases it is pure virtue. In having not only one *physical world* but many *virtual worlds* at ones disposal, the applicability range and precision to be expected from any model can, in principle, be tested very stringently. Unfortunately, in practice, such interaction between lattice practitioners and model builders is still rather under-developed for various psychological, communication-related and dogmatic reasons and, in some cases, even out of fear, mistrust or over-confidence, one might speculate.

The other way of *building bridges* is when a separation of scales occurs, in which the symmetries of QCD constrain the number of possible terms and allow for the systematic construction of an effective field theory. The most prominent examples are the chiral effective field theory ( $\chi$ EFT) that governs the low energy interactions of QCD as well as heavy quark effective theory (HQET) and non-relativistic QCD (NRQCD) for heavy quark physics. While in  $\chi$ EFT the scale separation occurs through the spontaneous breaking of the chiral symmetry by some collective gluonic effect, in HQET and NRQCD the scale separation is provided by the heavy quark mass  $m$ . Ideally, one would calculate the “high” energy Wilson coefficients of  $\chi$ EFT, such as the pion decay constant  $F_\pi$ , in lattice simulations (or determine them from fits to experimental data). The low energy expansion, as a function of  $m_\pi$ , can be determined analytically (chiral perturbation

theory). On the other hand, in HQET and NRQCD the low energy matrix elements can be provided by non-perturbative lattice simulations while the Wilson coefficients are calculable in perturbation theory, as long as  $m \gg \Lambda$ , where  $\Lambda$  denotes a typical non-perturbative scale of order 400 MeV.

It is this latter heavy quark limit, in which the static QCD potentials that are discussed here — as well as in Chapter 4 — can be related to mesonic bound states and, in the case of three body potentials, baryonic bound states. In doing this, QCD can be reduced to non-relativistic quantum mechanics within this particular sector, with the help of reasonable assumptions which themselves can be tested in lattice simulations. For example, in the case of quarkonia, QCD itself tells us what “potential model” we have to choose.

It is also possible to fit the spectra of light mesons and baryons, assuming phenomenological potentials. These potentials cannot be related in a systematic way either to QCD or to static potentials as calculated from Wilson loops. However, in spite of some rather dubious assumptions that are implicitly folded into such non-relativistic or relativized quark-potential models, it can still be instructive to compare the parametrizations that are commonly used in this context with those that are relevant in quarkonium physics. After all, most *physics* appears to interpolate smoothly between hadrons made out of light and heavy quarks. There also appears to be an intimate connection between, on one hand, the broken chiral symmetry that is most relevant in the light hadronic sector — but plays little direct rôle for quarkonia with masses much larger than the chiral symmetry breaking scale — and, on the other hand, the confining potential and flux tubes that seem to be the vacuum excitations that are responsible for interactions between the slowly moving heavy quark degrees of freedom.

## 1.2 The Static QCD Potential

The very definition of a “potential” requires the concept of “instantaneous” interactions: a test particle has to interact with the field induced by a source on a time scale short enough to guarantee that the relative distance remains unaffected. Whenever the relative speed of the two particles becomes relativistic, the underlying assumption of a constant time difference between cause and effect is obviously violated: only in non-relativistic systems, *i.e.* as long as the typical interaction energies ( $E$ ) within bound states are small

compared to the particle masses ( $M$ ), can we define a potential as a function of coordinates such as the distance  $r$ , the spin  $S$ , angular momentum  $L$  and relative momentum  $p$ . While for interactions between elementary charges in QED this is always the case as  $E/M = O(\alpha_F) \ll 1$ , QCD implies typical binding energies of order 400 MeV and only the bottom, and eventually the charm quark, can be regarded as non-relativistic.

Another example in which the non-relativistic approximation is justified are nucleon-nucleon potentials,  $V_{NN}(r)$ . Although there exist attempts to extract this information also from QCD, by employing lattice simulations (cf. Chapter 4 Subsec. 4.4.2), it is fair to predict that quantitatively reliable information, using the presently available methodology, might not become available within this decade. However, in this case a wealth of phenomenological information exists from experiment. For the quark-antiquark potential it is exactly the opposite. All experimental information is model dependent and rather indirect as quarks never appear as free particles in nature. However, this potential is among the most precisely determined quantities that have been calculated so far on the lattice

As a starting point one can make the test charges infinitely heavy, prohibiting any change in their relative speed and study the “static” limit. To this end we shall introduce the Wegner-Wilson loop and derive its relation to the static potential. Subsequently, expectations of this potential from exact considerations, strong coupling and string arguments as well as from perturbation theory are presented. Lattice results are then reviewed. Finally, the model is extended to non-static quarks and the form of the resultant potential in coordinate space is compared with its counterpart ( $\omega$ -meson exchange) in the nucleon-nucleon interaction.

### 1.2.1 *Wilson loops*

We will derive the relationship between the expectation values of Wegner-Wilson loops and the potential energy  $V(r) = E_0(r)$  between two colour charges, separated by a distance  $r$ . This is a technical but instructive exercise. The final result is displayed in Eq. 1.17.

The Wegner-Wilson loop was originally introduced by Wegner [1] as an order parameter in  $Z_2$  gauge theory. It is defined as the trace of the product of gauge variables  $U_{x,\mu}$  along a closed oriented contour  $\delta C$ , enclosing

an area  $C$ ,

$$W(C) = \text{Tr} \left\{ \mathcal{P} \left[ \exp \left( i \int_{\delta C} dx_\mu A_\mu(x) \right) \right] \right\} = \text{Tr} \left( \prod_{(x,\mu) \in \delta C} U_{x,\mu} \right). \quad (1.1)$$

While the loop, determined on a gauge configuration\*  $\{U_{x,\mu}\}$ , is in general complex, its expectation value is real, due to charge invariance: in Euclidean space we have  $\langle W(C) \rangle = \langle W^*(C) \rangle = \langle W(C) \rangle^*$ . It is straight forward to generalise the above Wilson loop to any non-fundamental representation  $D$  of the gauge field, just by replacing the variables  $U_{x,\mu}$  with the corresponding links  $U_{x,\mu}^D$ . The arguments below, relating the Wilson loop to the potential energy of static sources, go through independent of the representation according to which the sources transform under local gauge transformations. In what follows, we will denote a Wilson loop, enclosing a rectangular contour with one purely spatial distance,  $\mathbf{r}$ , and one temporal separation,  $t$ , by  $W(\mathbf{r}, t)$ . Examples of Wilson loops on a lattice for two different choices of contours  $\delta C$  are displayed in Figure 1.1.

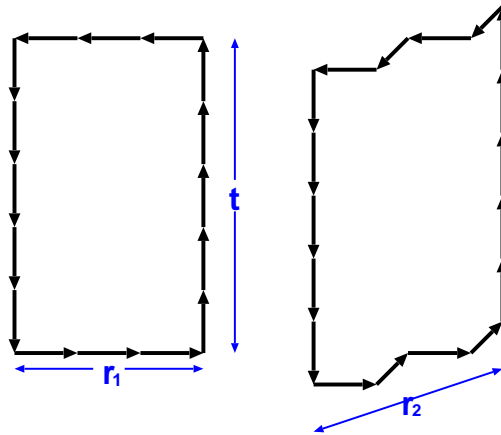


Fig. 1.1 Examples of rectangular on- and off-axis Wilson loops with temporal extent  $t = 5a$  and spatial extents  $r_1 = 3a$  and  $r_2 = 2\sqrt{2}a$ , respectively.

\* $U_\mu \in SU(3)$  a gauge group element, pointing into direction  $\mu \in \{1, 2, 3, 4\}$ , located between positions  $x$  and  $x + a\hat{\mu}$ , where  $a$  is the lattice spacing and  $x$  is a lattice point within the (finite) 4-volume.

In Wilson's original work [2], the Wilson loop had been related to the potential energy of a pair of static colour sources by using transfer matrix arguments. However, it took a few years until Brown and Weisberger attempted to derive the connection between the Wilson loop and the effective potential between heavy, not necessarily static, quarks in a mesonic bound state [3]. Later on, mass dependent corrections to the static potential have been derived along similar lines [4, 5] and the approach has been made systematic within the framework of EFTs [6, 7, 8, 9]. In Sec. 1.3, we will discuss these developments in more detail. Here, we derive the connection between a Wilson loop and the static potential between colour sources which highlights similarities with the situation in classical electrodynamics.

For this purpose we start from the Euclidean Yang-Mills action,

$$S = \frac{1}{4g^2} \int d^4x F_{\mu\nu}^a F_{\mu\nu}^a. \quad (1.2)$$

The canonically conjugated momentum to the field,  $A_i^a$ , is given by the functional derivative,

$$\pi_i^a = \frac{\delta S}{\delta(\partial_4 A_i^a)} = \frac{1}{g^2} F_{4i}^a = -\frac{1}{g} E_i^a. \quad (1.3)$$

The anti-symmetry of the field strength tensor implies  $\pi_4^a = 0$ . In order to obtain a Hamiltonian formulation of the gauge theory, we fix the temporal gauge *i.e.*  $A_4^a = 0$ . In infinite volume such gauges can always be found. On a toroidal lattice this is possible up to one time slice  $t'$ , which we demand to be outside of the Wilson loop contour, *i.e.*  $t' > t$ .

The canonically conjugated momentum,

$$\pi_\mu^a = -i \frac{\delta}{\delta A_\mu^a}, \quad (1.4)$$

now fulfils the usual commutation relations,

$$[A_j^a, \pi_\mu^b] = i \delta_{j\mu} \delta^{ab}, \quad (1.5)$$

and we can construct the Hamiltonian,

$$H = \int d^3x \left( \pi_\mu^a \partial_4 A_\mu^a - \frac{1}{4g^2} F_{\mu\nu}^a F_{\mu\nu}^a \right) = \frac{1}{2} \int d^3x (E_i^a E_i^a - B_i^a B_i^a) \quad (1.6)$$

that acts onto states  $\Psi[A_\mu]$ . In the Euclidean metric the magnetic contribution to the total energy is negative. Note that we can also add a fermionic

term  $\sum_f \bar{q}_f [\gamma_\mu D_\mu + m_f] q_f$  to the action above. In this case the momentum conjugate to the Dirac spinor field  $q_f^\alpha$  is given by  $-i\delta/\delta q_f^\alpha = \bar{q}_f^\alpha \gamma_4$ , where  $\alpha = 1, \dots, N_C$  runs over the colour in the fundamental representation. Here  $f$  denotes the quark flavour and  $m_f$  the respective mass.

A gauge transformation  $\Omega$  can be represented as a bundle of  $SU(N_C)$  matrices in some representation  $R$ ,  $\Omega_R(\mathbf{x}) = e^{i\omega^a(\mathbf{x})T_R^a}$ . We wish to derive the operator representation of the group generators  $T_R^a$ , that acts on the Hilbert space of wave functionals. For this purpose we start from the definition

$$R(\Omega)\Psi = \left[ 1 + i \int d^3x \omega^a(\mathbf{x}) T_R^a(\mathbf{x}) + \dots \right] \Psi = \Psi + \delta\Psi. \quad (1.7)$$

One easily verifies that  $\delta A_i = A_i^\Omega - A_i = -(\partial_i \omega + i[A_i, \omega]) \equiv D_i \omega(\mathbf{x})$ . We then obtain

$$\begin{aligned} \delta\Psi &= \int d^3x \delta A_i(\mathbf{x}) \frac{\delta\Psi}{\delta A_i(\mathbf{x})} = \int d^3x D_i \omega(\mathbf{x}) \frac{\delta\Psi}{\delta A_i(\mathbf{x})} \\ &= -\frac{i}{g} \int d^3x \omega^a(\mathbf{x}) (D_i E_i)^a(\mathbf{x}) \Psi, \end{aligned} \quad (1.8)$$

where we have performed a partial integration and have made use of the equivalence

$$\frac{\delta}{\delta A_i} = -\frac{i}{g} E_i \quad (1.9)$$

of Eqs. 1.3 and 1.4. Hence we obtain the representation

$$T_R^a = -\frac{1}{g} (D_i E_i)^a, \quad (1.10)$$

*i.e.* the covariant divergence of the electric field operator is the generator of gauge transformations! Again note that had we included sea quarks into the action, we would have encountered an additional term  $-\frac{1}{g} \sum_f \bar{q}_f \gamma_4 T^a q_f$  on the right hand side of this equation, where the generator is to be taken in the fundamental representation. It is trivial to generalize the equations below accordingly and the physical meaning is clear too: the vacuum has an intrinsic charge density distribution due to sea quarks. This then in turn allows for *string breaking* of the static potential.

Let us assume that the wave functional is a singlet under gauge transformations  $R(\Omega)\Psi[A_\mu] = \Psi[A_\mu]$ . This implies that

$$(D_i E_i)^a \Psi = 0, \quad (1.11)$$

which is Gauss' law in the absence of sources:  $\Psi$  lies in the eigenspace of  $D_i E_i$  that corresponds to the eigenvalue zero. Let us next place an external source in the fundamental representation of the colour group at position  $\mathbf{r}$ . In this case, the associated wave functional  $\Psi_\alpha, \alpha = 1, \dots, N_C$  transforms in a non-trivial way, namely

$$[R(\Omega)\Psi]_\alpha = \Omega_{\alpha\beta} \Psi_\beta. \quad (1.12)$$

This implies that

$$(D_i E_i)^a \Psi = -g\delta^3(\mathbf{r})T^a \Psi, \quad (1.13)$$

which again resembles Gauss' law, this time for a point-like colour charge at position<sup>†</sup>  $\mathbf{r}$ . For non-fundamental representations  $D$ , Eq. 1.13 remains valid under the replacement  $T^a \rightarrow T_D^a$ .

Let us now place a fundamental source at position  $\mathbf{0}$  and an anti-source at position  $\mathbf{r}$ . The wave functional  $\Psi_{\mathbf{r}}$ , which is an  $N_C \times N_C$  matrix in colour space will transform according to

$$\Psi_{\mathbf{r},\alpha\beta}^\Omega = \Omega_{\alpha\gamma}(\mathbf{0})\Omega_{\beta\delta}^*(\mathbf{r})\Psi_{\mathbf{r},\gamma\delta}. \quad (1.14)$$

One object with the correct transformation property is a gauge transporter (Schwinger line) from  $\mathbf{0}$  to  $\mathbf{r}$ ,

$$\Psi_{\mathbf{r}} = \frac{1}{\sqrt{N_C}} U^\dagger(\mathbf{r}, t) = \frac{1}{\sqrt{N_C}} \mathcal{P} \left[ \exp \left( i \int_0^{\mathbf{r}} d\mathbf{x} \mathbf{A}(\mathbf{x}, t) \right) \right], \quad (1.15)$$

which on the lattice corresponds to the ordered product of link variables along a spatial connection between the two points. Since we are in the temporal gauge,  $A_4(x) = 0$ , the correlation function between two such lines at time-like separation  $t$  is the Wilson loop

$$\langle W(\mathbf{r}, t) \rangle = \frac{1}{N_C} \langle U_{\alpha\beta}(\mathbf{r}, t) U_{\beta\alpha}^\dagger(\mathbf{r}, 0) \rangle, \quad (1.16)$$

<sup>†</sup>Of course, on a torus, such a state cannot be constructed. Note that in our Euclidean space-time conventions Gauss' law reads  $[\mathbf{D}\mathbf{E}]^a(\mathbf{x}) = -\rho^a(\mathbf{x})$ , where  $\rho$  denotes the charge density. Again note that, in general,  $\rho^a$  will automatically contain a contribution  $g\bar{q}_f \gamma_4 T_{\alpha f}$  for each sea quark flavour  $f$ .



which, being a gauge invariant object, will give the same result in any gauge. Other choices of  $\Psi_{\mathbf{r}}$ , *e.g.* linear combinations of spatial gauge transporters connecting  $\mathbf{0}$  with  $\mathbf{r}$ , define generalised (or smeared) Wilson loops,  $W_{\Psi}(\mathbf{r}, t)$ .

We insert a complete set of transfer matrix eigenstates,  $|\Phi_{\mathbf{r},n}\rangle$ , within the sector of the Hilbert space that corresponds to a charge and anti-charge in the fundamental representation at distance  $\mathbf{r}$ , and expect the Wilson loop in the limit of large temporal lattice extent,  $L_{\tau}a \gg t$ , to behave like

$$\langle W_{\Psi}(\mathbf{r}, t) \rangle = \sum_n |\langle \Phi_{\mathbf{r},n} | \Psi_{\mathbf{r}} | 0 \rangle|^2 e^{-E_n(\mathbf{r})t}, \quad (1.17)$$

where the normalisation convention is such that  $\langle \Phi_n | \Phi_n \rangle = \langle \Psi^\dagger \Psi \rangle = 1$  and the completeness of eigenstates implies  $\sum_n |\langle \Phi_n | \Psi | 0 \rangle|^2 = 1$ . Note that no disconnected part has to be subtracted from the correlation function since  $\Psi_{\mathbf{r}}$  is distinguished from the vacuum state by its colour indices.  $E_n(\mathbf{r})$  denote the energy levels. The ground state contribution  $E_0(\mathbf{r})$  — that will dominate in the limit of large  $t$  — can now be identified with the static potential  $V(\mathbf{r})$ , which we have been aiming to calculate.

The gauge transformation properties of the colour state discussed above, which determine the colour group representation of the static sources and their separation  $\mathbf{r}$ , do not yet completely determine the state in question: the sources will be connected by an elongated chromo-electric flux tube. This vortex can, for instance, be in a rotational state with spin  $\Lambda \neq 0$  about the inter-source axis. Moreover, under interchange of the ends the state can transform evenly ( $\eta = g$ ) or oddly ( $\eta = u$ ), where  $\eta$  denotes the combined  $CP$  parity. Finally, in the case of the one-dimensional  $\Lambda = 0$  representations, it can transform symmetrically or anti-symmetrically under reflections with respect to a plane containing the sources ( $\sigma_v = \pm$ ). It is possible to single out sectors within a given irreducible representation of the relevant cylindrical symmetry group [10],  $D_{\infty h}$ , with an adequate choice of  $\Psi$ . A straight line connection between the sources corresponds to the  $D_{\infty h}$  quantum numbers  $\Sigma_g^+$ , where  $\Lambda = 0, 1, 2, \dots$  is replaced by capital Greek letters,  $\Sigma, \Pi, \Delta, \dots$ . Any static potential that is different from the  $\Sigma_g^+$  ground state will be referred to as a “hybrid” potential. <sup>‡</sup> Since these potentials are gluonic excitations they can be thought of as being hybrids between pure “glueballs” and a pure static-static state; indeed, high hybrid excitations are unstable and will decay into lower lying potentials via the

<sup>‡</sup>Compare the discussion in Sec. 2.3.1 of Chapter 2

radiation of glueballs.

### 1.2.2 Exact results

We identify the static potential  $V(\mathbf{r})$  with the ground state energy  $E_0(\mathbf{r})$  of Eq. 1.17 that can be extracted from the Wilson loop of Eq. 1.1. By exploiting the symmetry of a Wilson loop under an interchange of the space and time directions, it can be proven that the static potential cannot rise faster than linearly as a function of the distance  $r$  in the limit  $r \rightarrow \infty$  [11]. Moreover, reflection positivity of Euclidean  $n$ -point functions [12, 13] implies convexity of the static potential [14], *i.e.*

$$V''(r) \leq 0. \quad (1.18)$$

The proof also applies to ground state potentials between sources in non-fundamental representations. However, it does not apply to hybrid excitations, since in this case the required creation operator extends into spatial directions, orthogonal to the direction of  $\mathbf{r}$ . Due to positivity, the potential is bound from below.<sup>§</sup> Therefore, convexity implies that  $V(r)$  is a monotonically rising function of  $r$ , *i.e.*

$$V'(r) \geq 0. \quad (1.19)$$

In Ref. [15], which in fact preceded Ref. [14], somewhat more strict upper and lower limits on Wilson loops, calculated on a lattice, have been derived: Let  $a_\sigma$  and  $a_\tau$  be temporal and spatial lattice resolutions. The main result for rectangular Wilson loops in representation  $D$  and  $d$  space-time dimensions then is

$$\langle W(a_\sigma, a_\tau) \rangle^{rt/(a_\sigma a_\tau)} \leq \langle W(r, t) \rangle \leq (1 - c)^{r/a_\sigma + t/a_\tau - 2}, \quad (1.20)$$

with  $c = \exp[-4(d-1)D\beta]$ . The resulting bounds on  $V(r)$  for  $r > a_\sigma$  read

$$-\ln(1 - c) \leq a_\tau V(r) \leq -\frac{r}{a_\sigma} \ln \langle W(a_\sigma, a_\tau) \rangle; \quad (1.21)$$

<sup>§</sup>The potential that is determined from Wilson loops depends on the lattice cut-off,  $a$ , and can be factorised into a finite potential  $\hat{V}(r)$  and a (positive) self energy contribution:  $V(r; a) = \hat{V}(r) + V_{\text{self}}(a)$ . The latter diverges in the continuum limit (see Sec. 1.2.5), whereas the potential  $\hat{V}(r)$  will become negative at small distances. Thus  $V(r; a)$  is indeed bounded from below by  $V(0)=0$ .

in consistency with Ref. [11], the potential (measured in lattice units  $a_\tau$ ) is bound from above by a linear function of  $r$  and it takes positive values everywhere.

### 1.2.3 Strong coupling expansions

Expectation values can be approximated by expanding the exponential of the lattice action, in terms of the inverse coupling  $\beta = 2N_C/g^2$ , giving  $\exp(-\beta S) = 1 - \beta S + \dots$ . This strong coupling expansion is similar to a high temperature expansion in statistical mechanics. When the Wilson action is used each factor  $\beta$  is accompanied by a plaquette and certain diagrammatic rules can be derived [2, 16, 17, 18, 19]. Let us consider a strong coupling expansion of the Wilson loop, Eq. 1.1. Since the integral over a single group element vanishes,

$$\int dU U = 0, \quad (1.22)$$

to zeroth order, we have  $\langle W \rangle = 0$ . To the next order in  $\beta$ , it becomes possible to cancel the link variables on the contour  $\delta C$  of the Wilson loop by tiling the whole minimal enclosed (lattice) surface  $C$  with plaquettes. Hence one obtains the expectation value [18, 20, 21, 22]

$$\langle W(C) \rangle = \left\{ \begin{array}{l} [\beta/4]^{-\text{area}(\delta C)} + \dots, \quad N_C = 2 \\ [\beta/2N_C^2]^{-\text{area}(\delta C)} + \dots, \quad N_C > 2 \end{array} \right\} \quad (1.23)$$

for  $SU(N_C)$  gauge theory. If we now consider the case of a rectangular Wilson loop that extends  $r/a$  lattice points into a spatial and  $t/a$  points into the temporal direction, we find the area law,

$$\langle W(\mathbf{r}, t) \rangle = \exp[-\sigma_d r t] + \dots, \quad (1.24)$$

with a string tension

$$\sigma_d a^2 = -d_r \ln \frac{\beta}{18}. \quad (1.25)$$

The numerical value of the denominator applies to  $SU(3)$  gauge theory; the potential is linear with slope  $\sigma_d$ , and so colour sources are confined at strong coupling. Here  $d_r = (|r_1| + |r_2| + |r_3|)/r \geq 1$  denotes the ratio between lattice and continuum norms and deviates from  $d_r = 1$  for source separations  $\mathbf{r}$  that are not parallel to a lattice axis. The string tension

of Eq. 1.25 depends on  $d_r$  and, therefore, on the lattice direction;  $O(3)$  rotational symmetry is explicitly broken down to the cubic subgroup  $O_h$ . The extent of violation will eventually be reduced as one increases  $\beta$  and considers higher orders of the expansion. Such high order strong coupling expansions have indeed been performed for Wilson loops [23] and glueball masses [24]. Unlike standard perturbation theory, whose convergence is known to be at best asymptotic [25, 26], the strong coupling expansion is analytic around  $\beta = 0$  [27] and, therefore, has a finite radius of convergence.

Strong coupling  $SU(3)$  gauge theory results seem to converge for  $\beta < 5$  — see, for example, Ref. [20]. One would have hoped to eventually identify a crossover region of finite extent between the validity regions of the strong and weak coupling expansions [28], or at least a transition point between the leading order strong coupling behaviour,  $a^2 \propto -\ln(\beta/18)$ , of Eq. 1.25 and the weak coupling limit,  $a^2 \propto \exp[-2\pi\beta/(3\beta_0)]$ , set by the asymptotic freedom of the QCD  $\beta$ -function. However, even after re-summing the strong coupling series in terms of improved expansion parameters and applying sophisticated Padé approximation techniques [29], nowadays such a direct crossover region does not appear to exist, necessitating one to employ Monte Carlo simulation techniques. In Fig. 1.2 we compare the strong coupling expansion for the string tension, calculated to  $O(g^{-24})$  *i.e.*  $O(\beta^{12})$  [23] with results from lattice simulations. While at large  $\beta$  the lattice results approach the weak coupling limit, there appears to be no overlap between weak and strong coupling and neither between strong coupling and lattice results in the region of interest ( $\beta \approx 6$  corresponds to a lattice spacing  $a^{-1} \approx 2$  GeV). We have taken the  $n_F = 0$  value of the QCD  $\Lambda$  parameter as determined non-perturbatively in Ref. [30] as normalization for the weak coupling expansion. The error band of the  $O(g^6)$  expectation is due to the corresponding statistical uncertainty. The  $O(g^4)$  central value lies within this band. There is no normalization ambiguity in the strong coupling results. Also at  $\beta > 5$ , the quality of convergence of the strong coupling expansion diminishes. This break-down might be related to a roughening transition that is discussed, for example, in Refs. [31, 32].

We would like to remark that the area law of Eq. 1.24 is a rather general result for strong coupling expansions in the fundamental representation of compact gauge groups. In particular, it applies also to  $U(1)$  gauge theory which we do not expect to confine in the continuum. In fact, based on duality arguments, Banks, Myerson and Kogut [33] have succeeded in proving

the existence of a confining phase in the four-dimensional theory and suggested the existence of a phase transition while Guth [34] has proven that, at least in the non-compact formulation of  $U(1)$ , a Coulomb phase exists. Indeed, in numerical simulations of (compact)  $U(1)$  lattice gauge theory two such distinct phases were found [35, 36], a Coulomb phase at weak coupling and a confining phase at strong coupling. The question whether the confinement one finds in  $SU(N_C)$  gauge theories in the strong coupling limit survives the continuum limit,  $\beta \rightarrow \infty$ , can at present only be answered by means of numerical simulation (and has been answered positively).

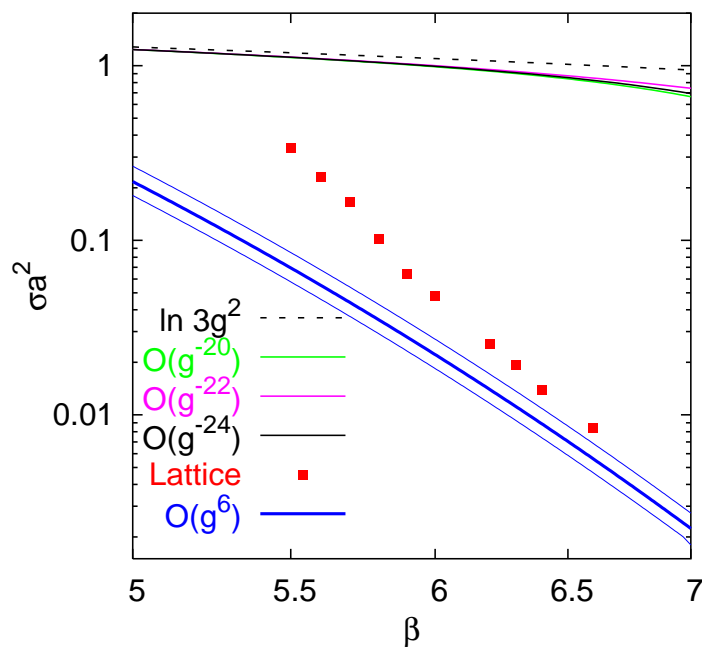


Fig. 1.2 Comparison of strong and weak coupling expansions with non-perturbative results for the string tension. The upper lines correspond to the strong coupling limit beginning with  $\ln 3g^2$  (dashed line) — the lowest order term from Eq. 1.25 for  $SU(3)$ . The other upper lines show the additional approximations up to  $O(g^{-24})$ . The lower lines correspond to the weak coupling limit up to  $O(g^6)$

### 1.2.4 String picture

The infra-red properties of QCD might be reproduced by effective theories of interacting strings. String models share many aspects with the strong coupling expansion. Originally, the string picture of confinement had been discussed by Kogut and Susskind [37] as the strong coupling limit of the Hamiltonian formulation of lattice QCD. The strong coupling expansion of a Wilson loop can be cast into a sum of weighted random deformations of the minimal area world sheet. This sum can then be interpreted to represent a vibrating string. The physical picture behind such an effective string description is that of the electric flux between two colour sources being squeezed into a thin, effectively one-dimensional, flux tube or Abrikosov-Nielsen-Olesen (ANO) vortex [38, 39, 40, 41]. As a consequence, this yields a constant energy density per unit length and a static potential that is linearly rising as a function of the distance.

One can study the spectrum of such a vibrating string in simple models [31, 42, 43]. Of course, the string action is not *a priori* known. The simplest possible assumption, employed in the above references, is that the string is described by the Nambu-Goto action [44, 45] in terms of  $d - 2$  free bosonic fields associated to the transverse degrees of freedom of the string. In this picture, the static potential is (up to a constant term) given by [42, 46]

$$V(r) = \sigma r \sqrt{1 - \frac{(d-2)\pi}{12\sigma r^2}} = \sigma r - \frac{(d-2)\pi}{24r} - \frac{(d-2)^2\pi^2}{1152\sigma r^3} - \dots \quad (1.26)$$

For a fermionic string [47] one would expect the coefficient of the correction term to the linear behaviour to be only one quarter as big as the Nambu-Goto one above. In the bosonic string picture, excited levels are separated from the ground state by

$$V_n^2(r) = V^2(r) + (d-2)\pi n\sigma = \left[ V(r) + \frac{(d-2)\pi n}{2r} - \dots \right]^2, \quad (1.27)$$

with  $n$  assuming integer values. It is clear from Eq. 1.26 that the string picture at best applies to distances

$$r \gg r_c = \sqrt{\frac{(d-2)\pi}{12\sigma}}. \quad (1.28)$$

For  $d = 4$  one obtains  $r_c \approx 0.33$  fm, when using the value  $\sqrt{\sigma} \approx 430$  MeV

from the  $\rho, a_2, \dots$  Regge trajectory.

The expectation of Eq. 1.26 has been very accurately reproduced in numerical simulations of  $Z_2$  gauge theory in  $d = 3$  space-time dimensions [48, 49]. In contrast, for  $d = 4$   $SU(3)$  gauge theory the spectrum of hybrid potentials still differs significantly from the expectation of Eq. 1.27 for distances as large as 2 fm [50, 51]. However, qualitatively the string picture is supported by the  $SU(3)$  data too, since the hybrid potentials at large  $r$  are found to group themselves into various bands that are separated by approximately equidistant gaps. These will eventually converge to values  $\pi/r$ , at even larger distances than accessible at present. Such an observation would support the existence of a bosonic string description of confining gauge theories in the very low energy regime [52, 53, 54, 55, 56]. Of course, in  $d < 26$ , the string Lagrangian is not renormalisable — but only effective — and higher order correction terms like torsion and rigidity will in general have to be added [57].

It is hard to disentangle in  $d = 4$  the (large distance)  $1/r$  term, expected from string vibrations, from the perturbative Coulomb term at short distances. However, a high precision attempt has been made recently, with promising results [58]. As an alternative, three-dimensional investigations (where perturbation theory yields a logarithmic contribution) have been suggested [59, 60]. Another way out is to determine the mass of a closed string, encircling a boundary of the lattice with a spatial extent  $l = L_\sigma a$  (a torelon), which is not polluted by a perturbative tail. The bosonic string expectation in this case would be [59]

$$E_n(l) = \sigma l - \frac{(d-2)\pi}{6l} + \dots \quad (1.29)$$

The naïve range of validity of the picture is  $l \gg l_c = 2r_c \approx 0.66$  fm. The numerical value applies to  $d = 4$  from Eq. 1.28. An investigation of the finite size dependence of the torelon mass in  $d = 4$   $SU(2)$  gauge theory has been performed some time ago by Michael and Stephenson [61] who found excellent agreement — on the 3 % level — with the bosonic string picture already for distances  $1 \text{ fm} \leq l \leq 2.4 \text{ fm}$ , quite close to  $l_c$ . Qualitative agreement has also been reported by Teper [62] from simulations of  $SU(2)$ ,  $SU(3)$ ,  $SU(4)$  and  $SU(5)$  gauge theories in three dimensions as well as in a recent study of four-dimensional  $SU(2N)$  gauge theories by Lucini *et al.* [63].

The bosonic string picture prediction of the free energy, calculated from

Polyakov line correlators, at finite temperatures  $T$  is similar to Eq. 1.29

$$-\frac{1}{\beta} \ln \langle P^*(r)P(0) \rangle = \sigma(\beta)r + \dots, \quad \sigma(T) = \sigma - \frac{(d-2)\pi}{6} T^2 + \dots, \quad (1.30)$$

with validity for  $r \gg T = aL_\tau$  [64]. The Polyakov line is defined as

$$P(\mathbf{x}) = \text{Tr} \left\{ \mathcal{T} \left[ \exp \left( i \int_0^{aL_\tau} dx_4 A_4(x) \right) \right] \right\} = \text{Tr} \left( \prod_{x_4=0}^{aL_\tau} U_{x,4} \right), \quad (1.31)$$

where  $\mathcal{T}$  denotes time ordering of the argument. The dependence of the effective string tension on the temperature has been checked for rather low  $T^{-1} < 1.24 T_c^{-1} \approx 0.93 \text{ fm}$  in studies of  $SU(3)$  gauge theory [65, 66]. Although the sign of the leading correction term to the zero temperature limit is correct, the difference comes out to be larger than predicted. It would be interesting to check whether the result will converge towards the string expectation at lower temperatures.

### 1.2.5 The potential in perturbation theory

The strong coupling expansion is specific to the lattice regularisation.<sup>¶</sup> However, the expectation value of a Wilson loop can also be approximated using standard perturbative techniques.

We will discuss the leading order weak coupling result that corresponds to single gluon exchange between two static colour sources which, although we neglect the spin structure, we will call “quarks” for convenience. From the Lagrangian,  $\mathcal{L}_{YM} = \frac{1}{2g^2} \text{Tr} F_{\mu\nu} F_{\mu\nu}$ , one can easily derive the propagator of a gluon with four-momentum  $q$ ,

$$G_{\mu\nu}^{ab}(q) = g^2 \frac{\delta^{ab} \delta_{\mu\nu}}{q^2}, \quad (1.32)$$

where  $\mu, \nu$  are Lorentz indices and  $a, b = 1, \dots, N_A$  label the colour generators with  $N_A^2 = N_C^2 - 1$  for  $SU(N_C)$ . The same calculation can be done starting from a lattice discretised action. The Wilson action yields the result of Eq. 1.32 up to the replacement

$$q_\mu \rightarrow \hat{q}_\mu = \frac{2}{a} \sin \left( \frac{aq_\mu}{2} \right). \quad (1.33)$$

<sup>¶</sup>However, new strong coupling methods have been developed in the large  $N_C$  limit, based on the Maldacena conjecture of QFT/AdS correspondence.



Other lattice actions yield slightly different results but they all approach Eq. 1.32 in the continuum limit,  $a \rightarrow 0$ . Momentum space potentials can be obtained from the on-shell static quark anti-quark scattering amplitude: the gluon interacts with two static external currents pointing into the positive and negative time directions,  $A_{\mu,\alpha\beta}^a = \delta_{\mu,4} T_{\alpha\beta}^a$  and  $A_{\nu,\gamma\delta}^b = -\delta_{\nu,4} T_{\gamma\delta}^b$ . Hence, we obtain the tree level interaction kernel

$$K_{\alpha\beta\gamma\delta}(q) = -\frac{g^2}{q^2} T_{\alpha\beta}^a T_{\gamma\delta}^a. \quad (1.34)$$

For sources in the fundamental representation, the Greek indices denote the colour indices of the external currents running from 1 to  $N_C$  and the quark anti-quark state can be decomposed into two irreducible representations of  $SU(N_C)$ ,

$$\mathbf{N}_C \otimes \mathbf{N}_C^* = \mathbf{1} \oplus \mathbf{N}_A. \quad (1.35)$$

We can now either start from a singlet or an octet<sup>||</sup> initial  $\Phi_{\beta\gamma} = Q_{\beta} Q_{\gamma}^*$  state,

$$\Phi_{\beta\gamma}^{\mathbf{1}} = \delta_{\beta\gamma}, \quad (1.36)$$

$$\Phi_{\beta\gamma}^{\mathbf{N}_A} = \Phi_{\beta\gamma} - \frac{1}{N_C} \delta_{\beta\gamma}, \quad (1.37)$$

where the normalisation is such that  $\Phi_{\alpha\beta}^i \Phi_{\beta\alpha}^j = \delta^{ij}$ . A contraction with the group generators of Eq. 1.34 yields

$$\Phi_{\beta\gamma}^{\mathbf{1}} T_{\alpha\beta}^a T_{\gamma\delta}^a = C_F \Phi_{\alpha\delta}^{\mathbf{1}}, \quad (1.38)$$

$$\Phi_{\beta\gamma}^{\mathbf{N}_A} T_{\alpha\beta}^a T_{\gamma\delta}^a = -\frac{1}{2N_C} \Phi_{\alpha\delta}^{\mathbf{N}_A}, \quad (1.39)$$

where  $C_F = N_A/(2N_C)$  is the quadratic Casimir charge of the fundamental representation.

We end up with the potentials in momentum space,

$$V_s(q) = -C_F g^2 \frac{1}{q^2}, \quad V_o(q) = \frac{g^2}{2N_C} \frac{1}{q^2} = -\frac{1}{N_A} V_s(q), \quad (1.40)$$

governing interactions between fundamental charges coupled to a singlet and to an octet, respectively: the force in the singlet channel is attractive while that in the octet channel is repulsive and smaller in size.

<sup>||</sup>We call the state  $\mathbf{N}_A$  an ‘‘octet’’ state, having the group  $SU(3)$  in mind.

How are these potentials related to the static position space inter-quark potential, defined non-perturbatively through the Wilson loop,

$$V(\mathbf{r}) = - \lim_{t \rightarrow \infty} \frac{d}{dt} \ln \langle W(\mathbf{r}, t) \rangle? \quad (1.41)$$

The quark anti-quark state creation operator,  $\Psi_{\mathbf{r}}$ , within the Wilson loop contains a gauge transporter and couples to the gluonic degrees of freedom. Thus, in general, it will have overlap with both,  $QQ^*$  singlet and octet channels\*\*. Since the singlet channel is energetically preferred, *i.e.*  $V_s < V_o$ , we might expect the static potential to correspond to the singlet potential. Up to order  $g^6$  this is indeed the case: to lowest order, the Wilson loop — defined by the closed contour  $\delta C$  — is given by the Gaussian integral

$$\langle W(\mathbf{r}, t) \rangle = \exp \left\{ -\frac{1}{2} \int d^4x d^4y J_\mu^a(x) G_{\mu\nu}^{ab}(x-y) J_\nu^b(y) \right\}, \quad (1.42)$$

where  $J_\mu^a = \pm T^a$  if  $(x, \mu) \in \delta C$  and  $J_\mu^a = 0$  elsewhere<sup>††</sup>. Eq. 1.42 implies for  $t \gg r$

$$\langle W(\mathbf{r}, t) \rangle = \exp \left( C_F g^2 t \int_{-t/2}^{t/2} dt' [G(\mathbf{r}, t') - G(\mathbf{0}, t')] \right). \quad (1.43)$$

We have omitted gluon exchanges between the spatial closures of the Wilson loop from the above formula. Up to order  $g^6$  (two loops), such contributions result in terms whose exponents are proportional to  $r$  and  $r/t$  and, therefore, do not affect the potential of Eq. 1.41. The propagator  $G_{\mu\nu}^{ab}(x)$ , the Fourier transform of  $G_{\mu\nu}^{ab}(q)$  in Eq. 1.32, contains the function

$$G(x) = \int \frac{d^4q}{(2\pi)^4} \frac{e^{iqx}}{q^2}, \quad \int_{-\infty}^{\infty} dx_4 G(x) = \frac{1}{4\pi} \frac{1}{r}. \quad (1.44)$$

After performing the  $t$ -integration, we obtain

$$V(\mathbf{r}, \mu) = -C_F \frac{\alpha_s}{r} + V_{\text{self}}(\mu), \quad (1.45)$$

\*\*Of course, for a quark and anti-quark being at different spatial positions, the singlet-octet classification should be consumed with caution in a non-perturbative context.

††Note that this formula, which automatically accounts for multi-photon exchanges, is exact in non-compact QED (excluding fermion loops) to any order of perturbation theory. However, in theories containing more complicated vertices, like non-Abelian gauge theories or compact lattice  $U(1)$  gauge theory, correction terms have to be added at higher orders in  $g^2$ .

where  $\alpha_s = g^2/(4\pi)$ . The piece

$$V_{\text{self}}(\mu) = C_F g^2 \int_{q \leq \mu} \frac{d^3 q}{(2\pi)^3} \frac{1}{q^2} = C_F \alpha_s \frac{2}{\pi} \mu, \quad (1.46)$$

that linearly diverges with the ultra-violet cut-off  $\mu$ , results from self-interactions of the static (infinitely heavy) sources. Comparing Eqs. 1.40 and 1.45 we indeed find

$$V(q) = V_s(q), \quad (1.47)$$

where

$$V(\mathbf{q}, 0) = \int d^3 r e^{i\mathbf{q}\cdot\mathbf{r}} \hat{V}(\mathbf{r}), \quad \hat{V}(\mathbf{r}) = V(\mathbf{r}, \mu) - V_{\text{self}}(\mu). \quad (1.48)$$

This self-energy “problem” is well known on the lattice and has also received attention in continuum QCD, in the context of renormalon ambiguities in quark mass definitions [67, 68].

Note that while  $V_s$  corresponds to the static potential, the perturbation theory relevant for hybrid excitations of the ground state potential corresponds to  $V_o$  [69].

At order  $\alpha_s^4$  a class of diagrams appears in a perturbative calculation of the Wilson loop that results in contributions to the static potential that diverge logarithmically with the interaction time [70]. In Ref. [71], within the framework of effective field theories, this effect has been related to ultra-soft gluons due to which an extra scale,  $V_o - V_s$ , is generated. Moreover, a systematic procedure has been suggested to isolate and subtract such terms to obtain finite singlet and octet interaction potentials between heavy quarks.

The logarithmic divergence is related to the fact that Eq. 1.43 contains an integration over the interaction time. For large times and any fixed distance  $r$ , Wilson loops will decay exponentially with  $t$ . However, the tree level propagator in position space is proportional to  $(r^2 + t^2)^{-1}$ , *i.e.* asymptotically decays like  $t^{-2}$  only. We notice that the integral receives significant contributions from the region of large  $t$  as demonstrated by the finite  $t \gg r$  tree level result

$$-\ln\langle W(r, t) \rangle = -\frac{C_F \alpha_s}{r} t \frac{2}{\pi} \left\{ \arctan \frac{t}{r} - \frac{r^2}{2t} \left[ \ln \left( 1 + \frac{t^2}{r^2} \right) \right] \right\} + (r + t) V_{\text{self}}. \quad (1.49)$$

The tree level lattice potential can easily be obtained by replacing  $q_\mu$  by  $\hat{q}_\mu$  from Eq. 1.33 and (in the case of finite lattice volumes) the integrals by discrete sums over lattice momenta,

$$q_i = \frac{2\pi}{L_\sigma} \frac{n_i}{a}, \quad n_i = -\frac{L_\sigma}{2} + 1, \dots, \frac{L_\sigma}{2}. \quad (1.50)$$

The lattice potential reads

$$V(\mathbf{r}) = V_{\text{self}}(a) - C_F \alpha_s \left[ \frac{1}{\mathbf{r}} \right], \quad (1.51)$$

where

$$\left[ \frac{1}{\mathbf{r}} \right] = \frac{4\pi}{L_\sigma^3 a^3} \sum_{\mathbf{q} \neq \mathbf{0}} \frac{e^{i\mathbf{q}\mathbf{r}}}{\sum_i \hat{q}_i \hat{q}_i} \quad (1.52)$$

and  $V_{\text{self}}(a) = C_F \alpha_s [1/\mathbf{0}]$ . We have neglected the zero mode contribution that is suppressed by the inverse volume  $(aL_\sigma)^{-3}$ . In the continuum limit,  $[1/\mathbf{r}]$  approaches  $1/r$  up to quadratic lattice artefacts whose coefficients depend on the direction of  $\mathbf{r}$  while  $V_{\text{self}}(a)$  diverges like

$$V_{\text{self}}(a) = C_F \alpha_s a^{-1} \times 3.1759115 \dots \quad (1.53)$$

The numerical value applies to the limit,  $L_\sigma \rightarrow \infty$ . Note that under the substitution  $\mu \approx 1.5879557 \pi/a$ , Eq. 1.53 is identical to Eq. 1.46. One loop computations of on-axis lattice Wilson loops can be found in Refs. [72, 73, 74], while off-axis separations in QCD with and without sea quarks have been realized in Ref. [75]. The tree level form, Eq. 1.51, is often employed to parameterise lattice artefacts — see Subsec. 5.9.3.1 of Chapter 5.

### 1.3 Quark-Antiquark Potentials between Non-Static Quarks

‡‡ So far in this chapter the rôle of the interquark potential has been to test various limits and models for QCD. For example, in Fig. 1.2 a comparison was made between the weak and strong coupling limits of QCD and also with the corresponding lattice results. Likewise, in Subsec. 1.2.4 string models were compared with the infra-red properties of QCD. This rôle

‡‡At this point the author “ran-out-of-steam” and so, because of the pressure of time, the editor felt that this chapter should be rapidly concluded — a task carried out by the editor himself with the semi-approval of the author.

is in stark contrast to that of the Nucleon-Nucleon potential  $[V(NN)]$  in nuclear physics, where  $V(NN)$  is mainly used as a stepping stone to the understanding of multi-nucleon systems. To this end, the many parameters needed to define  $V(NN)$  are first adjusted, more or less freely, to fit two nucleon experimental data, with — in some cases — values being imposed from meson-nucleon data or theories. Unlike  $V(Q\bar{Q})$ , the NN-potential is not able to predict reliable quantitative information about the input parameters to its theory — the only exception perhaps being an estimate of the  $\pi NN$  coupling constant [76]. The reason why the form of  $V(NN)$  is so complicated compared with that so far discussed for  $V(Q\bar{Q})$ , *i.e.* essentially  $V_{Q\bar{Q}}(r) = -e/r + cr$ , is because the latter is the interaction between two *static* quarks. If, however, we go away from this limit, then immediately the spins of the quarks begin to play a rôle resulting in forms similar to those encountered in  $V(NN)$ . These potentials should be reliable for describing  $b\bar{b}$ ,  $b\bar{c}$  and  $c\bar{c}$  states, since the  $b$  and  $c$  quarks are still sufficiently heavy ( $\approx 4.5$  and  $1.2$  GeV respectively) to not require a relativistic treatment. However, as soon as  $s$ ,  $d$ ,  $u$  quarks are involved, relativistic effects become important and even the whole concept of an interquark potential should be questioned. Furthermore, the hope that this potential between *two* quarks can account for multiquark systems has yet to be justified. Even so, this has not deterred its use as an effective interaction — a topic discussed in Chapter 5.

### 1.3.1 Radial form of $V(Q\bar{Q})$

What is the form of  $V(Q\bar{Q})$ ? To this question there is no unique answer, since — as with meson-exchange models of  $V(NN)$  — forms depend on the theory from which the potential is derived and in which it should be utilized. A good example of this ambiguity is the momentum dependence of the potential. Even though the correct relativistic scattering equation for two quarks is the Bethe-Salpeter equation, for practical reasons, this needs to be simplified to, say, the semi-relativistic Blankenbecler-Sugar or non-relativistic Schrödinger equations — see Subsec. 5.1.2.2 of Chapter 5 for a very brief discussion of this. If the basic Blankenbecler-Sugar equation is used directly then the appropriate potential contains relativistic factors of the form  $E_Q = \sqrt{M^2 + p^2}$ , where  $p$  is the momentum of the quark with mass  $M$ . However, it is often convenient to expand these momentum factors in powers of  $p/M$  resulting in a potential appropriate for a Lippmann-

Schwinger or Schrödinger approach.

Just as the interaction between two static quarks contained two distinct parts — *i.e.* the gluon exchange term  $V_G = -\frac{4}{3}\alpha_s/r$  and the confining term  $V_C = cr$  — so can the interaction between a heavy quark of mass  $M$  and an anti-quark of mass  $m$  be expressed as

$$V(Mm) = V_G(Mm) + V_C(Mm), \quad (1.54)$$

where

$$V_G(Mm)\left(-\frac{4}{3}\alpha_s\right)^{-1} = \frac{1}{r} - \frac{2\pi}{3Mm}\delta^{(3)}(r)\boldsymbol{\sigma}_M \cdot \boldsymbol{\sigma}_m - \frac{1}{4Mmr^3}S_{12} \\ - \frac{1}{2r^3} \left[ \frac{M^2 + m^2}{2M^2m^2} + \frac{2}{Mm} \right] \mathbf{L} \cdot \mathbf{S} + \frac{1}{8r^3} \frac{M^2 - m^2}{M^2m^2} (\boldsymbol{\sigma}_M - \boldsymbol{\sigma}_m) \cdot \mathbf{L} + \dots, \quad (1.55)$$

obtained by a non-relativistic reduction of the one-gluon-exchange mechanism and

$$V_C(Mm) = cr - \frac{c}{r} \frac{M^2 + m^2}{4M^2m^2} \mathbf{L} \cdot \mathbf{S} + \frac{c}{r} \frac{M^2 - m^2}{8M^2m^2} (\boldsymbol{\sigma}_M - \boldsymbol{\sigma}_m) \cdot \mathbf{L} + \dots. \quad (1.56)$$

These expressions for  $V_G(Mm)$  and  $V_C(Mm)$  do not include effects from expanding the  $E = \sqrt{M^2 + p^2}$  terms mentioned above — see, for example, Ref. [80]. Also here, for simplicity, they do not include spin-independent terms proportional to  $p^2$  and  $\delta^{(3)}(r)$ , since their form becomes ambiguous when going from a momentum space to a coordinate space representation. It should be added that it is convenient to have  $V_G(Mm)$  in coordinate space, since it is hard to deal with the linearly rising term  $cr$  from  $V_C(Mm)$  in momentum space. In addition to this ambiguity there are three others that enter in practice:

- (1) A crucial term in Eq.1.55 is the hyperfine interaction proportional to  $\boldsymbol{\sigma}_M \cdot \boldsymbol{\sigma}_m$ , which splits the energies of pseudoscalar and vector mesons. However, it is seen that it is proportional to  $\delta(\mathbf{r})$  — a radial form that needs to be regulated before it can be used in a wave-equation. This can be accomplished in a variety of ways, of which the most simple is to make the replacement

$$\delta(\mathbf{r}) \rightarrow \frac{a^3}{\pi^{3/2}} \exp(-a^2r^2) \quad (1.57)$$

as was done in the original work of Godfrey and Isgur [77]. Another approach is to consider this term as an effective interaction that is added in first order perturbation theory using those wavefunctions generated by the rest of  $V(Q\bar{Q})$ . In this case the overall constant is considered to be essentially a free parameter although reasonable estimates can be made from models involving instantons [78].

- (2) In Eq. 1.45,  $\alpha_s$  is the quark-gluon running coupling "constant" *i.e.* it depends on momentum  $k$ . This can be parameterised in a variety of ways *e.g.* from Ref. [79]

$$\alpha_s(k^2) = \frac{12\pi}{27} \frac{1}{\ln[(k^2 + 4m_g^2)/\Lambda^2]}, \quad (1.58)$$

where there are two parameters

- i) the gluon effective mass parameter  $m_g \approx 240$  MeV and
- ii) the QCD scale parameter  $\Lambda \approx 280$  MeV.

In Ref. [80] this is combined with the regulator of  $\delta(\mathbf{r})$  by the replacement

$$\alpha_s \delta(\mathbf{r}) \rightarrow \frac{1}{2\pi^2 r} \int_0^\infty dk k \sin(kr) \left( \frac{M+m}{E_M + E_m} \right) \left( \frac{Mm}{E_M E_m} \right) \alpha_s(k^2), \quad (1.59)$$

where  $E_M = \sqrt{M^2 + (k^2/4)}$  and  $E_m = \sqrt{m^2 + (k^2/4)}$ .

- (3) In the above it is implicitly assumed that  $V_C(Mm)$  is purely *scalar*. However, there are reasons — both theoretical and phenomenological — suggesting that there could be a sizeable *vector* component. For example, the spin-orbit splitting from  $V_G(Mm)$  is  $\propto 1/r^3$ , whereas that in  $V_C(Mm)$  is  $\propto -1/r$ . This indicates that the natural spin-orbit ordering of a coulomb-like potential should be inverted for high partial waves — a feature not seen experimentally or in lattice calculations. This is discussed in Subsec. 5.9.3.2 in Chapter 5.

Lattice calculations are able to isolate several of the components in the potential  $V(Mm)$  in Eq. 1.54. For example, the leading confinement term  $V_C(Mm) = cr$  of Eq. 1.56 is shown in Fig. 1.3. Another point of interest in this figure is that there is no sign of the expected flattening at  $r/r_0 \approx 2.4$ , where it becomes energetically favourable to create two mesons — denoted by the horizontal band [81]. For other components of the potential the lattice data is less precise, but still there is reasonable agreement with the

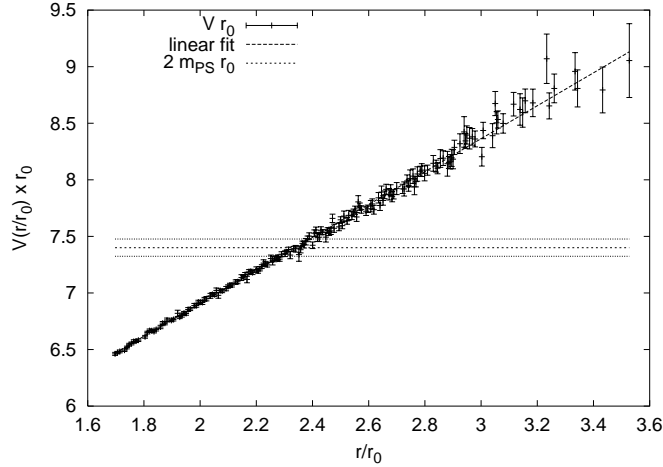


Fig. 1.3 The linearly rising confinement as calculated on a lattice [81] compared with  $V_C(Mm) = cr$  in Eq. 1.56.

expectations from Eqs. 1.55 and 1.56. Probably the most extensive lattice study of the various forms contained in the potential appear in Ref. [8].

### 1.3.2 Comparison with the form of $V(NN)$

For those more familiar with internucleon potentials it may be of interest to compare the forms that appear in  $V(NN)$  with those in  $V(Q\bar{Q})$ . This is, probably, best done by writing down explicitly the  $\omega$ -meson contribution to the familiar One-Boson-Exchange-Potential, since this meson is the one that resembles most closely a gluon both being vector particles independent of isospin/flavour. In  $V(NN)$ , the  $\omega$ -meson contributes much of the short range repulsion and also has a strong Spin-orbit potential. The form given in Ref. [82] is

$$\begin{aligned} \frac{V_\omega}{g^2} = & \frac{\exp(-\bar{m}r)}{r} - \frac{1}{2M^2} \left[ \nabla^2 \frac{\exp(-\bar{m}r)}{r} + \frac{\exp(-\bar{m}r)}{r} \nabla^2 \right] \\ & + \frac{1}{2M^2} \left[ \bar{m}^2 \frac{\exp(-\bar{m}r)}{r} - 4\pi\delta^{(3)}(r) \right] \left( 1 + \frac{\boldsymbol{\sigma}_1 \cdot \boldsymbol{\sigma}_2}{3} \right) \end{aligned}$$



$$-\frac{\bar{m}^2}{4M^2} \left[ \frac{1}{3} + \frac{1}{\bar{m}r} + \frac{1}{(\bar{m}r)^2} \right] \frac{\exp(-\bar{m}r)}{r} S_{12} + \frac{3}{2} \frac{1}{M^2} \frac{1}{r} \frac{d}{dr} \left[ \frac{\exp(-\bar{m}r)}{r} \right] \mathbf{L} \cdot \mathbf{S}, \quad (1.60)$$

where  $M$  is the nucleon mass and  $\bar{m} = 783 \text{ MeV} \approx 4\text{fm}^{-1}$  is the mass of the  $\omega$ . When  $\bar{m} \rightarrow 0$  to compare with one-gluon-exchange, this reduces to

$$\begin{aligned} \frac{V(m \rightarrow 0)}{g^2} &= \frac{1}{r} - \frac{1}{2M^2} \left[ \nabla^2 \frac{1}{r} + \frac{1}{r} \nabla^2 \right] - \frac{2\pi}{M^2} \delta^{(3)}(r) \left[ 1 + \frac{\boldsymbol{\sigma}_1 \cdot \boldsymbol{\sigma}_2}{3} \right] \\ &\quad - \frac{1}{4M^2} \frac{1}{r^3} S_{12} - \frac{3}{2} \frac{1}{M^2} \frac{1}{r^3} \mathbf{L} \cdot \mathbf{S}. \end{aligned} \quad (1.61)$$

This form is now quite similar to the one-gluon-exchange potential  $V_G$  in Eq. 1.55 — the only differences being the appearance of the spin-independent terms containing  $\nabla^2$  and  $\delta^{(3)}(r)$ , which are not unique in going from momentum space to coordinate space. Of course, it is possible to stay throughout in momentum space, since — unlike  $V_C(Mm)$  — here there is no linearly rising potential  $cr$ . However, there are also differences in how Eqs. 1.55 and 1.60 are treated. Normally in Eq. 1.60 the  $\delta^{(3)}(r)$  terms do not appear, since there are physically motivated models of form factors at the  $NN\omega$ -vertices, which smooth out such singularities. Also the results are not crucially dependent on these form factors since the main rôle of the  $\omega$ -meson is to generate a strong spin-isospin independent *repulsion* that essentially excludes the  $NN$ -wavefunction from the region of the origin. In contrast, the one-gluon-exchange potential in Eq. 1.55 has an *attractive* spin-isospin independent term ( $-\frac{4}{3}\alpha_s/r$ ). This means that uncertainties in the parametrizations in Eqs. 1.57 and 1.58 are more important.

#### 1.4 Conclusions

This chapter has attempted to describe a few of the many topics that could be covered by the title. It has not aimed at being in anyway comprehensive — the selection being rather subjective with the following ideas in mind.

1) The chapter began and ended with the theme that the interquark potential  $V(Q\bar{Q})$  could be viewed as a bridge for modelling QCD with somewhat the same rôle that the nucleon-nucleon potential  $V(NN)$  plays in nuclear physics. To further bring out the analogy between  $V(Q\bar{Q})$  and  $V(NN)$  the

radial forms were compared and contrasted in Sec. 1.3. However, it should be added that this possible “interdisciplinary bridge” is not well understood and its study is rather neglected.

2) The potential  $V(Q\bar{Q})$  can be used for testing approximations to QCD and its lattice formulation. This is illustrated in Fig. 1.2, where it is shown that the weak and strong coupling limits *do not* overlap for the energy range of interest *i.e.* between 100 MeV and a few GeV. Furthermore, over this range neither limit agrees with the corresponding (non-perturbative) lattice calculation. This feature shows that we are “forced” into performing lattice calculations, since there seems to be no other way of treating QCD with the couplings of most interest.

Here no mention has been made about deriving a discretized form of  $V(Q\bar{Q})$ . This topic has been the scene of much activity and comes under the heading of Non-Relativistic QCD (NRQCD). Here an expansion is made in terms of  $\Lambda/M_Q$  with  $\Lambda \sim 1$  GeV being a characteristic energy scale for non-perturbative effects. A few comments can be found in Subsec. 5.1.2.1 of Chapter 5.

### Acknowledgements

I express sincere gratitude to Tony Green, for his initiative in suggesting this book and in particular for his patience in waiting for a ridiculously long time for my contribution to arrive. Discussions with Nora Brambilla, Antonio Pineda, Joan Soto and Antonio Vairo are acknowledged. I received support from a PPARC Advanced Fellowship (grant PPA/A/S/2000/00271) as well as by PPARC grant PPA/G/0/2002/0463.

### Bibliography

- [1] F. J. Wegner, *J. Math. Phys.*, 12:2259, 1971.
- [2] K. G. Wilson, *Phys. Rev.*, D10:2445, 1974.
- [3] L. S. Brown and W. I. Weisberger, *Phys. Rev.*, D20:3239, 1979.
- [4] E. Eichten and F. L. Feinberg, *Phys. Rev. Lett.*, 43:1205, 1979.  
E. Eichten and F. L. Feinberg, *Phys. Rev.*, D23:2724, 1981.
- [5] A. Barchielli, E. Montaldi and G. M. Prospero, *Nucl.Phys.*, B296:625,1988,  
*erratum, ibid.* B303:752,1988  
A. Barchielli, N. Brambilla and G. M. Prospero, *Nuovo Cim.* A103:59,1990

- [6] A. Pineda and A. Vairo *Phys. Rev.*, D63:054007, 2001.
- [7] Yu-Qi Chen, Yu-Ping Kuang, and R. J. Oakes, *Phys. Rev.*, D52:264, 1995.
- [8] G. S. Bali, K. Schilling, and A. Wachter, *Phys. Rev.*, D56:2566, 1997.
- [9] N. Brambilla, A. Pineda, J. Soto, and A. Vairo, *Phys. Rev.*, D63:014023, 2001
- [10] L. D. Landau and E. M. Lifschitz. *Lehrbuch der theoretischen Physik, Band 3: Quantenmechanik*, Akademie Verlag, Berlin, DDR, 1979.
- [11] E. Seiler, *Phys. Rev.*, D18:482, 1978.
- [12] K. Osterwalder and R. Schrader, *Commun. Math. Phys.*, 31:83, 1973.
- [13] K. Osterwalder and R. Schrader, *Commun. Math. Phys.*, 42:281, 1975.
- [14] C. Bachas, *Phys. Rev.*, D33:2723, 1986.
- [15] B. Simon and L. G. Yaffe, *Phys. Lett.*, 115B:145, 1982.
- [16] K. G. Wilson, *Phys. Rept.*, 23:331, 1976.
- [17] R. Balian, J. M. Drouffe, and C. Itzykson, *Phys. Rev.*, D11:2104, 1975, *erratum*, *ibid.* D19:2514, 1979.
- [18] M. Creutz, *Rev. Mod. Phys.*, 50:561, 1978.
- [19] J. M. Drouffe and J. B. Zuber, *Phys. Rept.*, 102:1, 1983.
- [20] M. Creutz, *Quarks, Gluons and Lattices*. Cambridge University Press, Cambridge, UK, 1983.
- [21] I. Montvay and G. Münster, *Quantum fields on a lattice*. Cambridge University Press, Cambridge, UK, 1994.
- [22] J. Smit, Introduction to quantum fields on a lattice: A robust mate, *Cambridge Lect. Notes Phys.*, 15:1, 2002.
- [23] G. Münster and P. Weisz, *Phys. Lett.*, 96B:119, 1980. *erratum*, *ibid.* 100B:519, 1981.
- [24] G. Münster, *Nucl. Phys.*, B190:439, 1981. *errata*, *ibid.* B200:536, 1982 and B205:648, 1982.
- [25] F. J. Dyson, *Phys. Rev.*, 85:631, 1952.
- [26] J. Zinn-Justin, *Phys. Rept.*, 70:109, 1981.
- [27] K. Osterwalder and E. Seiler, *Ann. Phys.*, 110:440, 1978.
- [28] J. B. Kogut and J. Shigemitsu, *Phys. Rev. Lett.*, 45:410, 1980.
- [29] J. Smit, *Nucl. Phys.*, B206:309, 1982.
- [30] S. Capitani, M. Lüscher, R. Sommer, and H. Wittig, *Nucl. Phys.*, B544:669, 1999.
- [31] M. Lüscher, *Nucl. Phys.*, B180:317, 1981.
- [32] J. M. Drouffe and J. B. Zuber, *Nucl. Phys.*, B180:264, 1981.
- [33] T. Banks, R. Myerson, and J. Kogut, *Nucl. Phys.*, B129:493, 1977.
- [34] A. H. Guth, *Phys. Rev.*, D21:2291, 1980.
- [35] M. Creutz, L. Jacobs, and C. Rebbi, *Phys. Rev.*, D20:1915, 1979.
- [36] B. Lautrup and M. Nauenberg, *Phys. Lett.*, 95B:63, 1980.
- [37] J. Kogut and L. Susskind, *Phys. Rev.*, D11:395, 1975.
- [38] A. A. Abrikosov, *Sov. Phys. JETP*, 5:1174, 1957.
- [39] H. B. Nielsen and P. Olesen, *Nucl. Phys.*, B61:45, 1973.
- [40] G. 't Hooft, *Nucl. Phys.*, B72:461, 1974.

- [41] A. A. Migdal, *Phys. Rept.*, 102:199, 1983.
- [42] M. Lüscher, K. Symanzik, and P. Weisz, *Nucl. Phys.*, B173:365, 1980.
- [43] M. Lüscher, G. Münster, and P. Weisz, *Nucl. Phys.*, B180:1, 1981.
- [44] T. Goto, *Prog. Theor. Phys.*, 46:1560, 1971.
- [45] Y. Nambu, *Phys. Rev.*, D10:4262, 1974.
- [46] J. F. Arvis, *Phys. Lett.*, 127B:106, 1983.
- [47] M. Caselle, R. Fiore, and F. Gliozzi, *Phys. Lett.*, B200:525, 1988.
- [48] M. Caselle, R. Fiore, F. Gliozzi, M. Hasenbusch, and P. Provero, *Nucl. Phys.*, B486:245, 1997.
- [49] M. Caselle, M. Hasenbusch, and M. Panero, *JHEP*, 01:057, 2003.
- [50] C. J. Morningstar, K. J. Juge, and J. Kuti, *Nucl. Phys. Proc. Suppl.*, 73:590, 1999.
- [51] K. Jimmy Juge, J. Kuti, and C. Morningstar, QCD string formation and the Casimir energy, hep-lat/0401032
- [52] E. T. Akhmedov, M. N. Chernodub, M. I. Polikarpov, and M. A. Zubkov, *Phys. Rev.*, D53:2087, 1996.
- [53] A. M. Polyakov, *Nucl. Phys.*, B486:23, 1997.
- [54] M. N. Chernodub and D. A. Komarov, *JETP Lett.*, 68:117, 1998.
- [55] D. Antonov and D. Ebert, *Phys. Lett.*, B444:208, 1998.
- [56] M. Baker and R. Steinke, *Phys. Lett.*, B474:67, 2000.
- [57] J. Polchinski and A. Strominger, *Phys. Rev. Lett.*, 67:1681, 1991.
- [58] M. Luscher and P. Weisz, *JHEP*, 07:049, 2002.
- [59] J. Ambjørn, P. Olesen, and C. Peterson, *Nucl. Phys.*, B244:262, 1984.
- [60] P. Majumdar, *Nucl. Phys.*, B664:213, 2003.
- [61] C. Michael and P. W. Stephenson, *Phys. Rev.*, D50:4634, 1994.
- [62] M. J. Teper, *Phys. Rev.*, D59:014512, 1999.
- [63] B. Lucini, M. Teper, and U. Wenger, Glueballs and k-strings in SU(N) gauge theories : calculations with improved operators, hep-lat/0404008 .
- [64] P. de Forcrand, G. Schierholz, H. Schneider, and M. Teper, *Phys. Lett.*, 160B:137, 1985.
- [65] O. Kaczmarek, F. Karsch, E. Laermann, and M. Lütgemeier, *Phys. Rev.*, D62:034021, 2000.
- [66] O. Kaczmarek, S. Ejiri, F. Karsch, E. Laermann, and F. Zantow, Heavy quark free energies and the renormalized Polyakov loop in full QCD, hep-lat/0312015.
- [67] I. I. Bigi, M. A. Shifman, N. G. Uraltsev, and A. I. Vainshtein, *Phys. Rev.*, D50:2234, 1994.
- [68] M. Beneke, *Phys. Lett.*, B434:115, 1998.
- [69] G. S. Bali and A. Pineda, *Phys. Rev.*, D69:094001, 2004.
- [70] T. Appelquist, M. Dine, and I. J. Muzinich, *Phys. Lett.*, 69B:231, 1977.
- [71] N. Brambilla, A. Pineda, J. Soto, and A. Vairo, *Phys. Rev.*, D60:091502, 1999.
- [72] G. Curci, G. Paffuti, and R. Tripiccion, *Nucl. Phys.*, B240:91, 1984.
- [73] R. Wohlert, P. Weisz, and Werner Wetzel, *Nucl. Phys.*, B259:85, 1985.

- [74] U. Heller and F. Karsch, *Nucl. Phys.*, B251:254, 1985.
- [75] G. S. Bali and P. Boyle, Perturbative Wilson loops with massive sea quarks on the lattice, hep-lat/0210033.
- [76] V. Stoks, R. Timmermans and J. J. de Swart, *Phys. Rev.*, C47:512, 1993, nucl-th/9211007
- [77] S. Godfrey and N. Isgur, *Phys. Rev.*, D32:189, 1985.
- [78] S. Chernyshev, M. A. Nowak, and I. Zahed, *Phys. Rev.*, D53:5176, 1996.
- [79] A. C. Mattingly and P. M. Stevenson, *Phys. Rev.*, D49:437, 1994.
- [80] T. A. Lähde, C. J. Nyfält and D. O. Riska, *Nucl. Phys.*, A674:141, 2000, hep-ph/9908485
- [81] B. Bolder *et al.*, *Phys. Rev.*, D63:074504, 2001.
- [82] R. Bryan and B.L. Scott, *Phys. Rev.*, 177:1435, 1969.